Numerical Simulation of the Howard Street Tunnel Fire, Baltimore, Maryland, July 2001

Kevin B. McGrattan
Anthony Hamins

Numerical Simulation of the Howard Street Tunnel Fire, Baltimore, Maryland, July 2001

Kevin B. McGrattan
Anthony Hamins
Fire Research Division
Building and Fire Research Laboratory

August 2002

Abstract

This report documents a study undertaken to estimate the thermal environment of the Howard Street Tunnel in Baltimore, Maryland, following the derailment in July 2001 of a freight train and the burning of spilled tripropylene and the contents of surrounding rail cars. A numerical fire model developed by the National Institute of Standards and Technology (NIST) has been used to simulate the fire's growth and spread in the tunnel. The fire model has been validated for this application using temperature data collected during a series of fire experiments conducted at a decommissioned highway tunnel in West Virginia. The cross-sectional area of the tunnel and the fire sizes used in the West Virginia experiments are similar to the Howard Street Tunnel.

For the Howard Street Tunnel fire, the peak calculated temperatures within the tunnel were approximately 1,000 °C (1,800 °F) within the flaming regions, and on average approximately 500 °C (900 °F) when averaged over a length of the tunnel equal to three to four rail car lengths. Because of the insulation provided by the thick brick walls of the tunnel, the calculated temperatures within a few car lengths of the fire were relatively uniform, consistent with what one would expect to find in an oven or furnace. The peak wall surface temperature reached about 800 °C (1,500 °F) where the flames were directly impinging, and on average 400 °C (750 °F) over the length of three to four rail cars. The steel temperature of the rail cars would be expected to be similar to the surrounding gas temperature because of the long exposure time and the high thermal conductivity of steel.

Contents

List of Figures

1   Introduction

On July 18, 2001, at 3:08 pm, a 60 car CSX freight train powered by 3 locomotives traveling through the Howard Street Tunnel in Baltimore, Maryland, derailed 11 cars. A fire started shortly after the derailment. The tunnel is 2,650 m (8,700 ft, 1.65 mi) long with a 0.8 % upgrade in the section of the tunnel where the fire occurred. There is a single track within the tunnel. Its lower entrance (Camden portal) is near Orioles Park at Camden Yards; its upper entrance is at Mount Royal Station. The train was traveling towards the Mount Royal portal when it derailed. For almost its entire length the tunnel runs beneath Howard Street. A fire erupted under the intersection of Howard and Lombard Streets where a ruptured tank car (52nd out of 60 cars) spilled tripropylene onto the floor of the tunnel. It is unclear how the fire started, but it is speculated that a spark produced when the tank car was punctured could have been the cause. The liquid fuel sustained a fire that lasted several hours. It is believed that other materials burned slowly for several days within closed box cars. The other cars on the train were transporting a variety of bulk materials including pulp board, brick, steel, soy oil, paper, and a variety of corrosive acids.

Under the sponsorship of the US Nuclear Regulatory Commission (NRC), the Building and Fire Research Laboratory of the National Institute of Standards and Technology (NIST) has undertaken a study of the incident to assess the thermal environment within the tunnel during the fire. The National Transportation Safety Board (NTSB) has conducted an investigation of the tunnel fire and provided NIST with information about the tunnel, the damage to the rail cars, and various other details [1]. Using information collected at the scene by the NTSB, a series of numerical simulations has been performed to predict the temperature of the hot gases and the heat flux to various objects within the tunnel.

The simulations reported in this study are not intended to replicate every detail of the Howard Street Tunnel fire, since the information about the fuel spill, tunnel floor, track and ballast, *etc.*, is not known to a high enough level of certainty to permit an exact reconstruction of the event. The approach taken is to use what information is known about the incident as a starting point for the calculations, and then to vary the unknown parameters to ascertain the range in possible outcomes. This information is useful in assessing the risk to materials that are commonly transported by rail.

2   Technical Approach

In cooperation with the fire protection engineering community, a numerical fire model, Fire Dynamics Simulator (FDS), is being developed at NIST to study fire behavior and to evaluate the performance of fire protection systems in buildings. Version 2 of FDS was publicly released in December 2001 [2, 3]. The model is based on the low Mach number form of the Navier-Stokes equations and uses a large eddy simulation (LES) technique to represent unresolved, sub-grid scale motion. The fire is modeled by solving a transport equation for the conserved scalar quantity known as the mixture fraction, a linear combination of the fuel and oxygen that indicates the mass fraction of the gas originating as fuel. The advantage of the mixture fraction approach is that all of the species transport equations are combined into one, reducing the computational cost. Thermal radiation is modeled by solving the radiative transport equation for a non-scattering gray gas using what is known as the Finite Volume Method [4].

Improvements have been made to FDS version 2 to extend its range of application to include the long tunnel geometry and the under-ventilated fire conditions. The most important improvement for this problem is the addition of a multiblock meshing scheme. Originally, the FDS algorithm solved the fluid dynamic equations on a single rectangular uniform mesh that spanned the volume of interest. The problem with this approach is that too much computational time is wasted in regions that do not necessarily require high resolution. For example, when simulating the fire and smoke movement in a long tunnel, only the region near the fire needs to be covered with a fine numerical grid. The rest of the tunnel need not have such a fine grid. The use of multiple numerical grids of various spatial sizes allows the computational domain to be extended to accommodate the entire length of the tunnel, but still retain high accuracy near the fire.

The calculations to be discussed solve the mass, momentum and energy conservation equations on a computational grid whose cells are on the order of 15 cm to 30 cm (6 in to 1 ft) near the fire source. A coarse mesh is used farther from the fire where it is not as important to capture the detailed mixing of fuel and oxygen. The objective of the calculations is to estimate the temperatures within the tunnel, and the heat flux to surrounding objects. As a check on the numerical algorithm, several fire experiments for which temperature measurements are available have been simulated first to ensure that the numerical model is working properly, and that the chosen numerical grid is adequate.

FDS can provide valuable insight into how a fire may have developed. The model, however, is only a simulation. The model output is dependent on a variety of input values such as material properties, timelines, geometry, and ventilation openings. Since perfect knowledge of every detail of the fire site, fuel load or timeline is never known, estimations are incorporated into the model. To better understand the sensitivity of modeling results to variation of these parameters, a parametric study using FDS was performed. For example, a parametric study was conducted on the effect of the thermal conductivity of the bricks lining the tunnel, the size of the fuel spill, and the effect of the tunnel dimensions. These parametric studies are described in Section 6 of this report.

The ability of the FDS model to accurately predict the temperature and velocity of fire gases has been previously evaluated by conducting experiments, both lab-scale and full-scale, and measuring quantities of interest. For relatively simple fire-driven flows, such as buoyant plumes and flows through doorways, FDS predictions are within the experimental uncertainty of the values measured in the experiments [5]. In large-scale fire tests reported in Ref. [6], FDS temperature predictions were found to be within 15 % of the measured temperatures and the heat release rates

were within 20 % of the measured values. In full-scale tunnel fire tests, FDS simulations were within 50 °C (100 °F) of the peak measured values. The results in this report are presented as ranges to accommodate the uncertainties.

Further details on the numerical model may be found in the Appendix. A complete description of the numerical model can be found at the web site

`http://fire.nist.gov/fds`

3   Model Validation Studies

Two sets of calculations are included in this section to demonstrate the capabilities of the FDS model. The first set of calculations was performed to validate the model's ability to predict the movement of smoke and hot gases from a fire in a relatively large, open building. They are included here as an example of how the model is often used in practice by fire protection engineers. The FDS model is used by hundreds of engineers around the world, who constantly validate it for use in a wide variety of problems. These validation exercises raise the level of confidence in applying the model to fire scenarios that are different from those commonly seen in residential or industrial settings.

The geometry of the second validation exercise is directly related to the present study. It compares calculations to measurements for a set of fire experiments performed in a decommissioned highway tunnel in West Virginia. Although the tunnel is slightly larger in cross section than the Howard Street Tunnel, the temperatures measured during these experiments should not be significantly different from those experienced during the Howard Street Tunnel fire, and provide a useful check on the simulations to be performed for the current study.

3.1   Fire Model Evaluation for Nuclear Power Plant Applications

FDS has recently been applied to a series of benchmark fire tests performed as part of the *International Collaborative Project to Evaluate Fire Models for Nuclear Power Plant Applications* [7]. The tests analyzed were designated as Benchmark Exercise #2. Three fire experiments were performed in a large fire test hall. In each, a pool of heptane was burned for about 5 minutes, during which time gas temperatures were measured in three vertical arrays and at two points within the fire plume. The hall was 27 m (89 ft) long, 14 m (45 ft) wide and 19 m (62 ft) high with a sloped ceiling, an exhaust duct, and several doors opening near its base. The fire size and ventilation configurations were changed from test to test.

Figure 1 shows the geometry of the test hall and the layout of the various numerical grids used in the simulation. The finest grid surrounding the fire is 4 m by 4 m by 10 m high, with grid cells 13 cm on a side. Five other separate grids are used to cover the rest of the space at a resolution of 40 cm. Within each grid, the cells are uniform in size. In all, 216,000 grid cells are used in the calculation. Ten minutes of real time are simulated. Some simplifications to the geometry include making the burner and the exhaust duct square rather than round, and approximating the sloped ceiling as a series of stair steps. Because boundary layer effects were not considered important, these approximations did not impact the final results. Otherwise, everything else is as specified in the problem description. Heptane (C_7H_{16}) is used as a fuel. Temperature and velocity predictions are recorded at all of the specified locations.

The results of the calculations agree well with the measurements. An example of the results is shown in Fig. 2. The predicted temperatures at the 5 upper thermocouple locations in each array are within 10 °C of the measured temperatures, which are 100 to 150 °C above ambient. The lower 5 temperature locations show good agreement as well, with the greatest difference being for the lowest thermocouple, which under-predicts the measured temperatures by about 10 °C. The measured temperatures in the lower layer were 20 to 100 °C above ambient. Given slightly higher temperatures in the upper layer, it is not surprising to see slightly lower temperatures somewhere else since the model conserves energy. The model assumes that there is no air movement in the
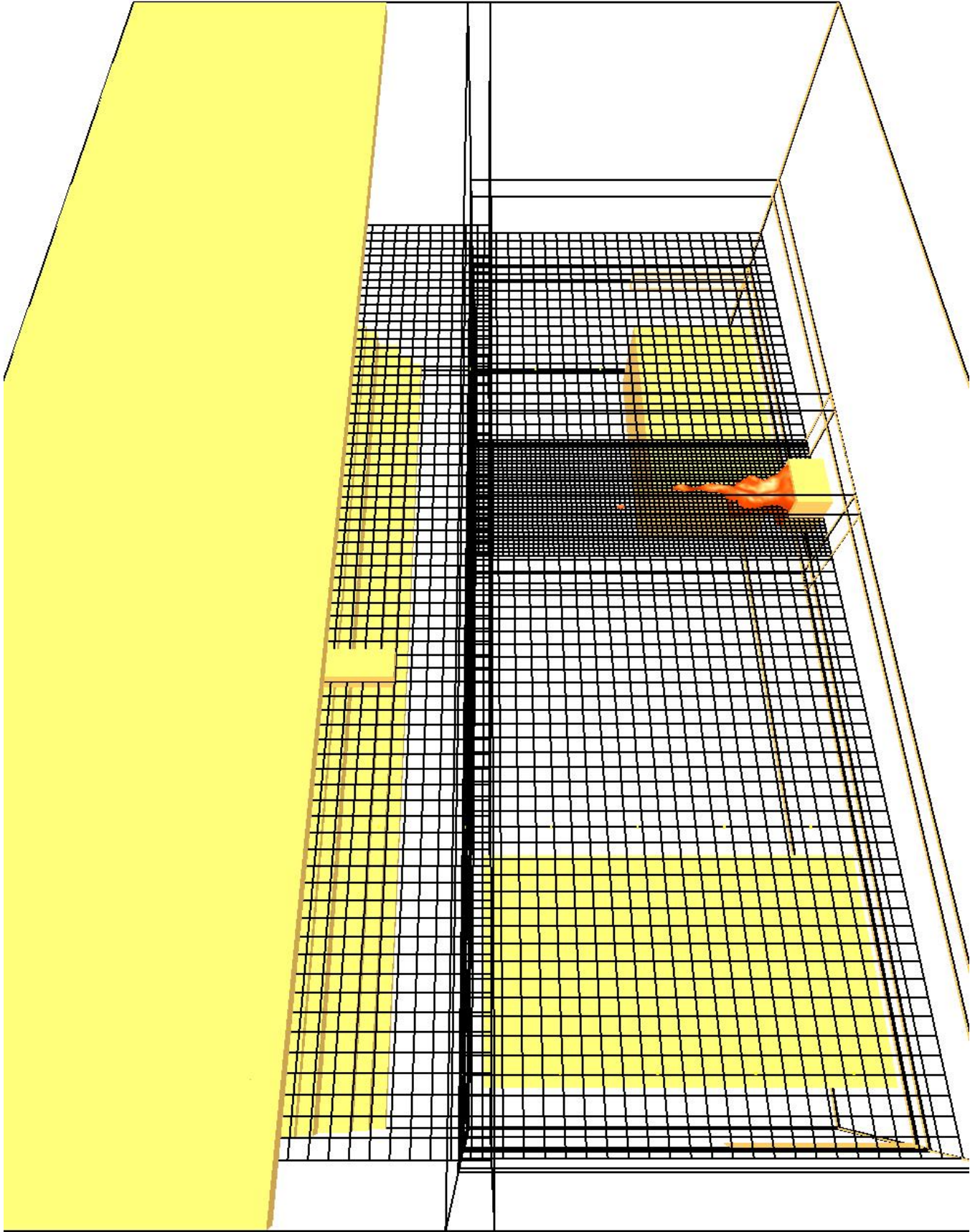
FIGURE 1: Geometry of the fire test hall used in the validation study, showing the various numerical grids used in the calculations.

hall except for that induced by the fire or the ventilation system, thus one would expect the level of mixing to be slightly under-predicted. Another source of uncertainty in the measurement is the absorption of thermal radiation by the thermocouples in the lower layer, leading to slightly higher thermocouple temperatures over the surrounding gas temperature.

The results of this exercise are very favorable. The numerical model works very well in situations where the heat release rate is known, and the fire has an adequate supply of oxygen, as in these tests. When the heat release rate is not known, and when the fire is not free to burn at its peak rate because of oxygen limitations, the results are subject to greater uncertainty, as in the next example.

FIGURE 2: Comparison of measured (circles) and predicted (lines) temperatures along a vertical rake of thermocouples in the center of a 19 m tall test hall. The peak heat release rate for the 10 min test was 3.8 MW. The thermocouples labeled T2.1 to T2.10 span the height of the hall from 2 m off the floor to 1 m below the ceiling.

3.2 Memorial Tunnel Fire Ventilation Test Program

The second validation exercise of the model involves one of a series of tunnel fire experiments conducted in a decommissioned highway tunnel in West V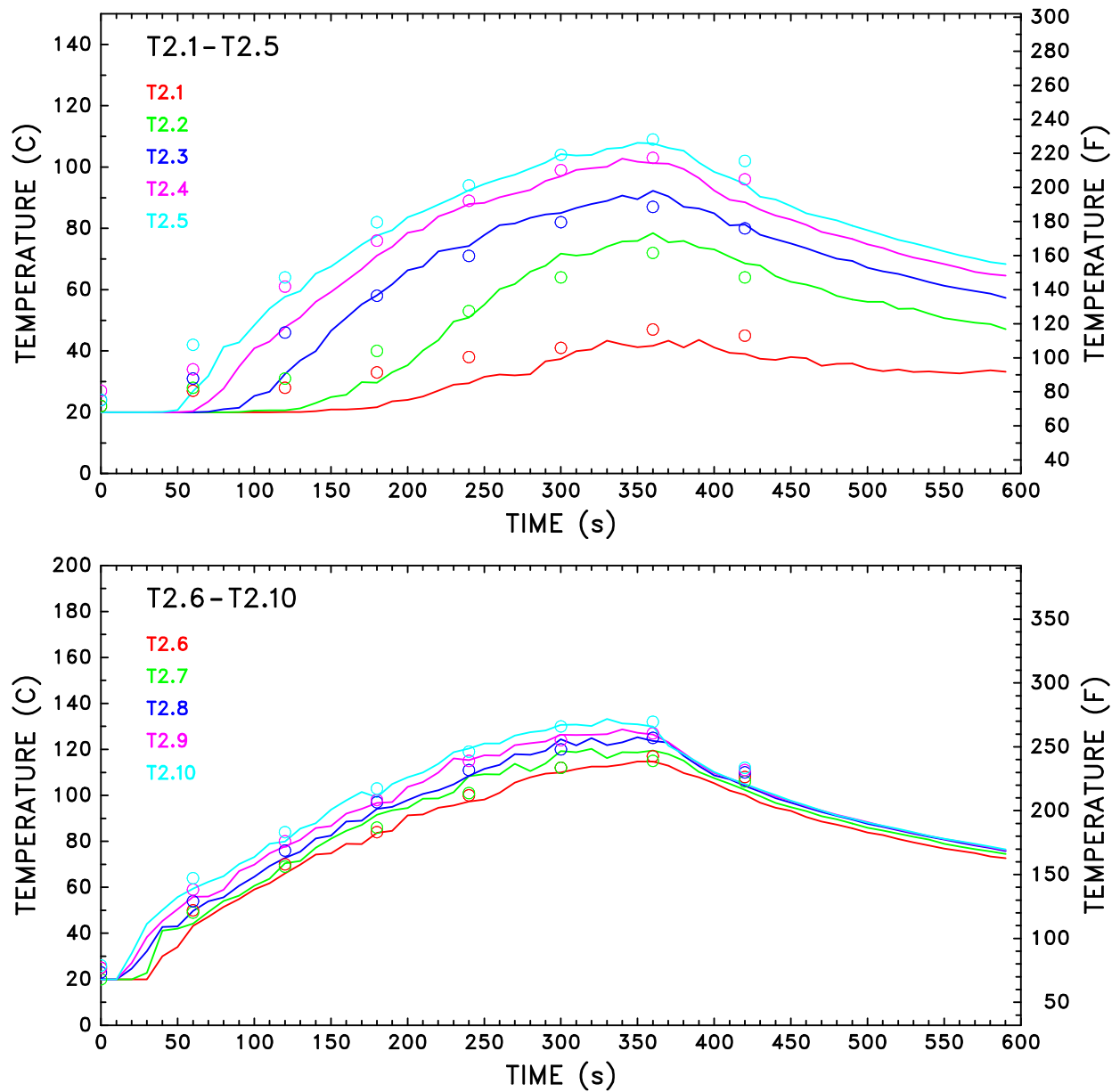irginia from 1993 to 1995 [8]. The tunnel is 853 m (2,800 ft) long with a 7.9 m (26 ft) ceiling height, a 3.2 % upgrade, and a semi-circular ceiling (see Fig. 3). A series of fire tests was conducted by Parsons Brinckerhoff in which various fire sizes and ventilation schemes were used. Of most relevance to the Howard Street Tunnel fire were tests with fire sizes of 20 MW and 50 MW and only natural ventilation. The fuel for the tests was No. 2 fuel oil poured on top of water in large pans. The fuel surface was about 0.6 m (2 ft) off the floor of the tunnel. The burning rate of fuel was not monitored during the tests. Instead, the pan size was chosen so that the burning rate would be approximately what was desired based on previously measured burning rates of the fuel.

The temperatures recorded near the ceiling of the tunnel directly over the fire during the 20 MW and 50 MW tests are considerably different. For the 20 MW test, the gas temperature over the fire reached approximately 300 °C (600 °F), whereas for the 50 MW test, the temperature reached approximately 800 °C (1,500 °F) during the 15 min burn period. The measured temperatures within the fire itself were similar in both tests.

For the 20 MW fire, Figures 4 and 5 show temperature contours along a vertical centerline plane at times of 5 min and 16 min past ignition of the fuel for both the experiments and the simulations. The tunnel has a 3.2 % upgrade (Howard Street Tunnel has a 0.8 % upgrade), which accounts for the smoke and heat moving to the left (uphill). Peak temperatures above the fire were measured to be about 320 °C (600 °F). The numerical simulation was conducted with a numerical grid whose cells are on the order of 30 cm (1 ft) for covering a 130 m (425 ft) section of the tunnel surrounding the fire pan. The peak temperatures agree to within 50 °C (100 °F). At the uphill end of the tunnel, the simulation under-estimates the extent of the lower temperature contours. For example, in Fig. 5, the 200 °F contour extends half way to the Fan Room over the left opening of the tunnel, whereas in the numerical simulation, this same temperature contour only extends about a quarter of the way. The reason for this difference is that the simulation employs coarser numerical grids at the ends of the tunnel since the objective of the calculations is to predict the thermal environment within 100 m of the fire.

For the 50 MW fire, Figures 6 and 7 show temperature contours along a vertical centerline plane at times of 3 and 14 minutes past ignition of the fuel for both the experiments and the simulations. Peak temperatures above the fire were measured to be about 800 °C (1,500 °F) in the first few minutes, decreasing to about 700 °C (1,300 °F) after 14 min. The slight reduction in peak temperatures most likely is due to the underventilated environment in the upper layer of the tunnel which restricts the fuel from burning close to the ceiling. In the numerical simulation, the peak temperature is within 50 °C (100 °F) of the experimental measurement. At the uphill end of the tunnel, the simulation under-estimates the extent of the lower temperature contours. For example, in Fig. 7, the 200 °F contour extends to the Fan Room over the left opening of the tunnel, whereas in the numerical simulation, this same temperature contour only extends about two-thirds of the way. The reason for this difference is that the simulation employs coarser numerical grids at the ends of the tunnel since the objective of the calculations is to predict with as much accuracy as possible the thermal environment within 100 m of the fire.
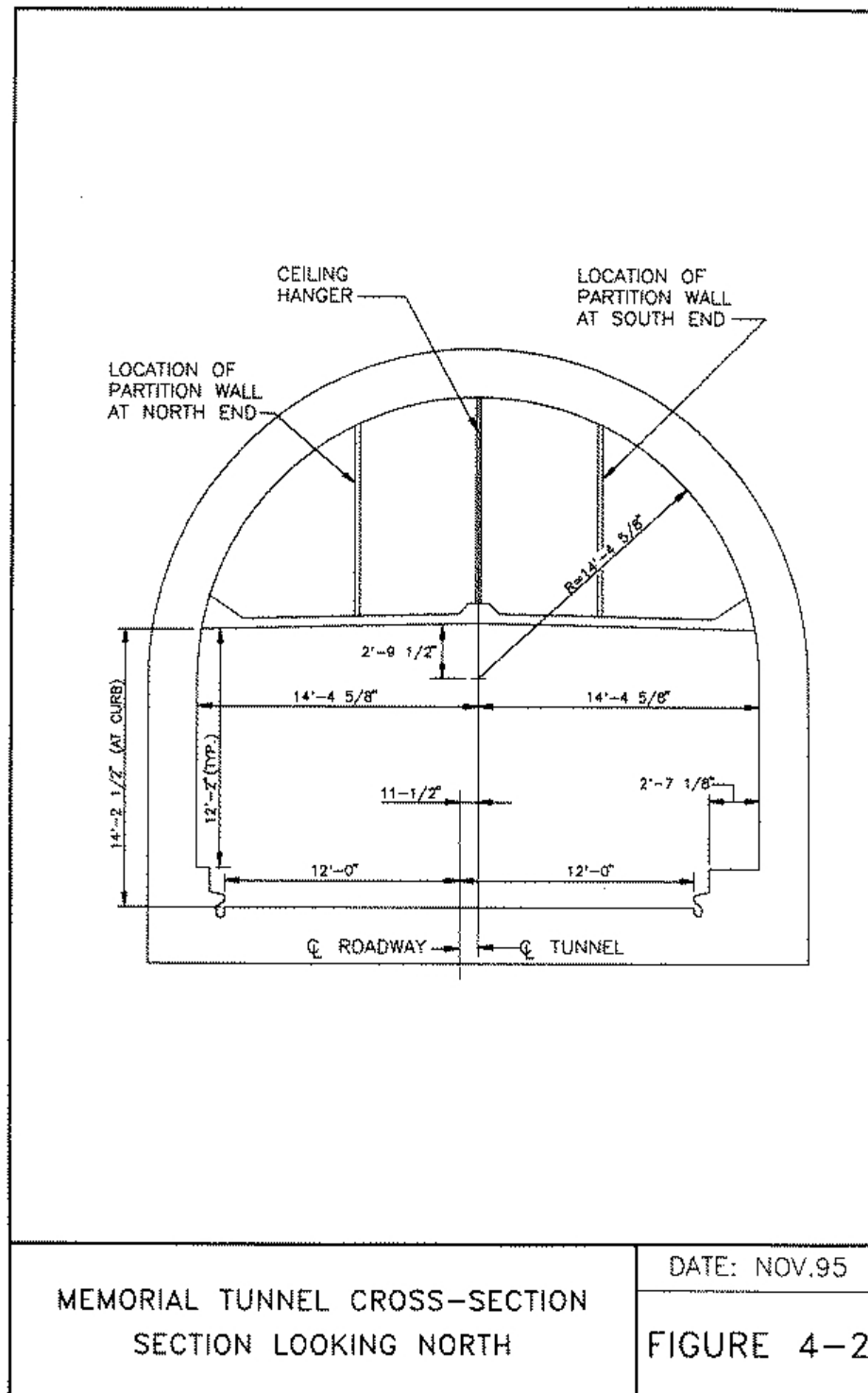
FIGURE 3: Cross section of Memorial Tunnel, West Virginia, reprinted from Reference [8]. Note that all lengths are reported in units of feet and inches. The height of the tunnel is 7.9 m (26 ft); its width is 8.8 m (29 ft). The tunnel walls and ceiling are constructed of concrete. In comparison, the Howard Street Tunnel in Baltimore is approximately 6.7 m (22 ft) high, 8.2 m (27 ft) wide, and lined with brick.

FIGURE 4: Temperatures along the centerline vertical plane during the 20 MW unventilated fire test performed as part of the Memorial Tunnel Fire Ventilation Test Program. Shown are the experimental (top figure) and predicted (lower figure) temperatures 5 minutes past ignition. The colored contours in the lower figure are at increments of 60 °F, starting at 60 °F which separates the light and dark blue regions. The red contours in the lower figure denote regions in excess of 300 °C (600 °F). The highest temperature contour in the upper figure is 600 °F over the fire near the ceiling. The tunnel is not shown to scale. The tunnel slopes upwards from right to left.

10

FIGURE 5: Temperatures along the centerline vertical plane during the **20 MW** unventilated fire test performed as part of the **Memorial Tunnel Fire Ventilation Test Program.** Shown are the experimental (upper figure) and predicted (lower figure) temperatures 16 minutes past ignition. The colored contours are at increments of 60 °F, starting at 60 °F which separates the light and dark blue regions. The red contours in the lower figure denote regions in excess of 300 °C (600 °F). The highest temperature contour in the upper figure is 500 °F. The tunnel is not shown to scale. The tunnel slopes upwards from right to left.

11
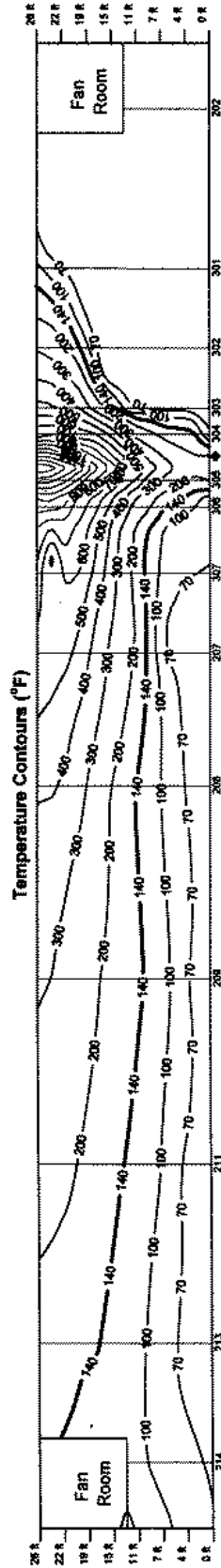
FIGURE 6: Temperatures along the centerline vertical plane during the 50 MW unventilated fire test performed as part of the Memorial Tunnel Fire Ventilation Test Program. Shown are the experimental (upper figure) and predicted (lower figure) temperatures 3 minutes past ignition. The colored contours are at increments of 100 °F, starting at 100 °F which separates the light and dark blue regions. The red contours in the lower figure denote regions in excess of 600 °C (1,100 °F). The highest predicted temperature is 750 °C (1,400 °F). The highest temperature contour in the upper figure is 1,500 °F. The tunnel is not shown to scale. The tunnel slopes upwards from right to left.
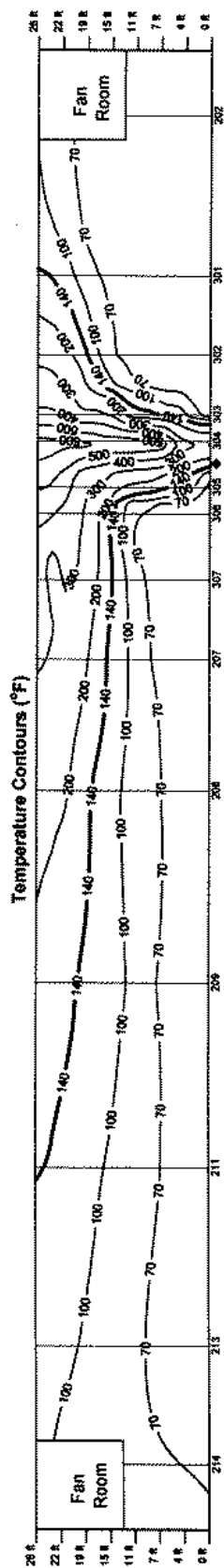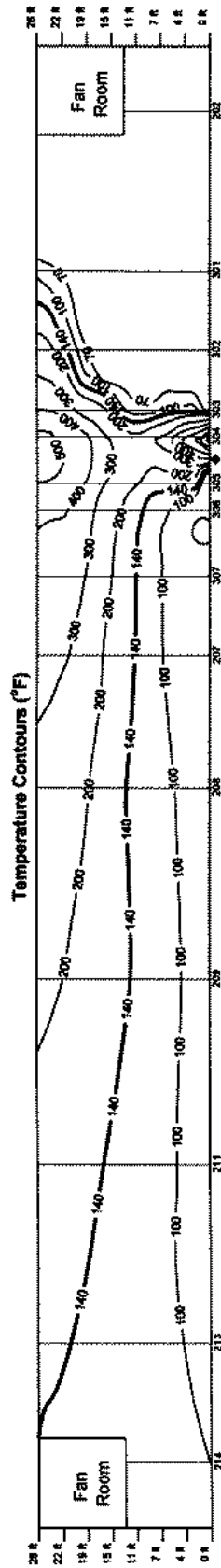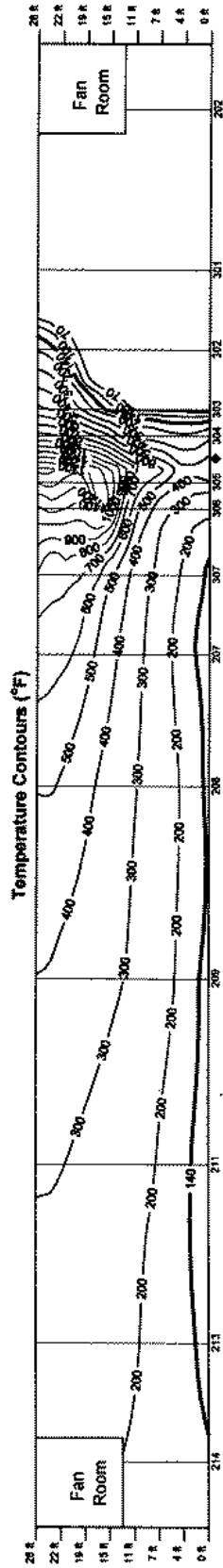
FIGURE 7: Temperatures along the centerline vertical plane during the 50 MW unventilated fire test performed as part of the Memorial Tunnel Fire Ventilation Test Program. Shown are the experimental (upper figure) and predicted (lower figure) temperatures 14 minutes past ignition. The colored contours are at increments of 100 °F, starting at 100 °F which separates the light and dark blue regions. The red contours in the lower figure denote regions in excess of 600 °C (1,100 °F). The peak predicted temperature is 700 °C (1,300°F). The highest experimental temperature contour is 1,300 °F. The tunnel is not shown to scale. The tunnel slopes upwards from right to left.

13

4   Howard Street Tunnel Fire Simulation Parameters

The comparison of the Memorial Tunnel Fire Test results with those of FDS supports the use of the model for the Howard Street Tunnel fire. In this section, we will discuss the various model inputs, with an emphasis on the similarities and differences between the Howard Street and Memorial Tunnel fires. Information about the accident has been provided by the National Transportation Safety Board in the form of photographs of the scene and sketches of the tunnels, Figs. 8 and 9.[1]

The overall geometry of the Memorial and Howard Street Tunnels is similar. Because of this, it is expected that the fire behavior in both would be similar. Both have barrel-shaped roofs, both are relatively small in cross-sectional area. The height of the Memorial Tunnel is 7.9 m (26 ft); its width is 8.8 m (29 ft). In comparison, the Howard Street Tunnel is approximately 6.7 m (22 ft) high, 8.2 m (27 ft) wide, although these dimensions vary over the length of the tunnel. In the vicinity of the fire, the Howard Street Tunnel is 6.4 m (21.0 ft) high and 9.9 m (32.5 ft) wide. The Memorial Tunnel is 850 m (2,800 ft, 0.53 mi) long, whereas the Howard Street Tunnel is 2,650 m (8,700 ft, 1.65 mi) long. The Memorial Tunnel has a 3.2 % upgrade; the Howard Street Tunnel has a 0.8 % upgrade in the section of the tunnel where the fire occurred. The 0.8 % upgrade persists until the Mount Royal portal (see Fig. 9).

The rail cars in the tunnel were assumed to be solid blocks 3.0 m (10 ft) wide and 4.0 m (13 ft) high with 1.0 m (3 ft) of void space beneath to represent the undercarriage. Most of the cars were centered in the tunnel, but several of the derailed cars were offset based on the diagram of the accident scene provided by the NTSB. The cars in the simulation served as targets of thermal radiation and obstructions limiting the airflow to the fire. Specific damage to the cars was not included in the simulations.

The fire in the Howard Street Tunnel is believed to have been fueled initially by spilled tripropylene. This liquid is assumed to consist mainly of nonene (C_9H_{18}, relative molecular mass 126 g/mol). Ideally, nonene burns according to the reaction

$$2\,C_9H_{18} + 27\,O_2 \rightarrow 18\,CO_2 + 18\,H_2O \tag{1}$$
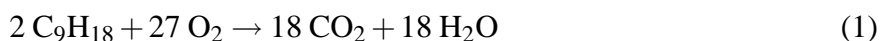
The heat of combustion for the reaction is ideally 44,300 kJ/kg, but is less in under-ventilated environments, where the production of soot and CO (among many other by-products of incomplete combustion) is substantial. Measurements of the exhaust gases from fully-involved room fire experiments show that the yields[2] of soot and CO are on the order of 0.2, although no data are available specifically for tripropylene/nonene [9]. The conversion of the carbon in the fuel into soot and CO, rather than CO_2, reduces the heat of combustion from its ideal value.

The pool of tripropylene was assumed to evaporate with a heat of vaporization of 300 kJ/kg and a boiling temperature of 135 °C [10]. The calculations were relatively insensitive to the exact value of these parameters because the fire was oxygen-limited. In other words, the fuel evaporated readily in the hot tunnel; there was more fuel vapor than there was oxygen to burn it. Changing the heat of vaporization and boiling temperature had little effect on the final results. More discussion of these types of parameter sensitivities can be found in the Analysis and Discussion (Section 6).

The tunnel was assumed to be lined with a meter-thick layer of brick. The number of courses (layers) of brick varied between 8 (36 in, 0.9 m) in the vicinity of the fire, and 5 (22.5 in, 0.6 m)

---

[1]These sketches may be difficult to read in printed form. The electronic version of the report contains the original images that can be enlarged to show detail.

[2]The *yield* of a combustion product is the mass of the product produced per unit mass of fuel burned

DERAILED CAR INFORMATION *

CAR NUMBER	WEIGHT (TONS)	CAR LENGTH (FT.)	CAR DESCRIPTION	HAZ. MAT. CODE	DERAILED STATUS
46	106	58	CSXT140140		DERAILED TO SOUTH SIDE
47	110	58	CSXT140092		DERAILED TO SOUTH SIDE
48	106	57	AN 5701		DERAILED, NOT SURE OF POSITION OF TRUCKS, TRAILING END STARTING TO LEAN TO NORTH WALL.
49	108	59	CSXT136353		DERAILED LEANING ON NORTH WALL
50	111	58	CSXT140341		DERAILED LEANING ON NORTH WALL
51	104	55	CSXT158745		DERAILED LEANING ON NORTH WALL
52	123	63	SRIX 30015	2057	DERAILED, B END TRUCK BACK UNDER CAR ABOUT 1/3 OF CAR LENTH. A END TRUCK MOVED BACK 12 TO 18 INCHES.
53	129	49	RCRX 1345	1789	DERAILED
54	131	53	RCRX 1072	1789	DERAILED
55	130	55	ETCX623504	8082	DERAILED
56	86	55	RBOX 43199		DERAILED EAST END

* DESCRIPTIONS PROVIDED BY CSXT.

DERAILMENT SKETCH

HOWARD STREET CURB LINE

NORTH TUNNEL WALL

SOUTH TUNNEL WALL

TUNNEL WIDTH APPROX. 26'

APPROX. CENTER LINE TRACK/TUNNEL

POINT OF DERAILMENT 62+23

HOLE IN WALL TUNNEL STA 62+40 APPROX. 1112 FT NORTH (RR EAST) OF M.P. 96

FEB 2000 WATER LEAK

40" WATER LINE

OPENING IN PAVEMENT

MANHOLE ACCESS

PLATFORM

BRK COMM EQUIP

LOMBARD ST.

HOWARD ST.

HOWARD STREET CURB LINE

TUNNEL STA. 65+00

CARS 60 THRU 57 REMOVED (RR WEST) PORTAL
APPROX. 2400' TO SOUTH (RR WEST) PORTAL

350' TO 400' TO CARS 43 THRU 1 TO NORTH
APPROX. 5800' TO NORTH (RR EAST) PORTAL

WEST

EAST

CAR NO. 46
CAR NO. 47
CAR NO. 48
CAR NO. 49
CAR NO. 50
CAR NO. 51
CAR NO. 52
CAR NO. 53
CAR NO. 54
CAR NO. 55
CAR NO. 56

B END
A END

NOTES:
DIMENSIONS SHOWN ARE APPROXIMATE.
THE TRAIN POSITION, AS REPORTED ON THE CSXT TRAIN DOCUMENTATION, INCLUDES THREE LOCOMOTIVES, 60 CARS TOTAL.
TUNNEL STA. 0+00 AT NORTH (RR EAST) PORTAL.

FIGURE 8: Sketch of Howard Street Tunnel and derailed cars, courtesy of the National Transportation Safety Board.
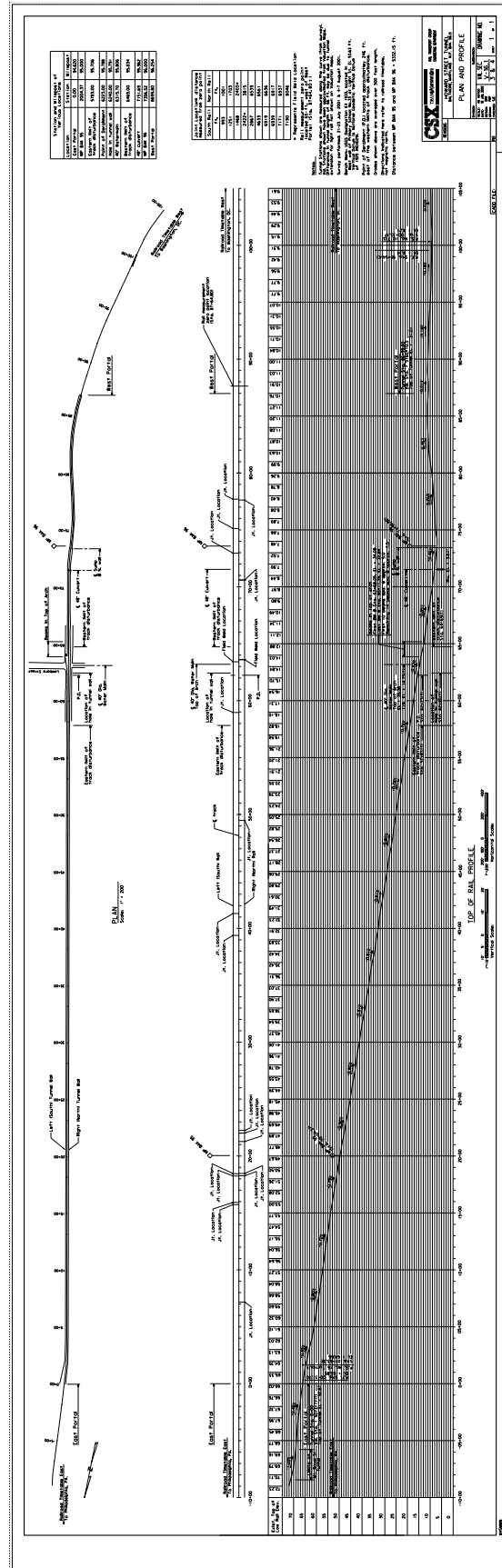
FIGURE 9: Elevation diagram of Howard Street Tunnel, courtesy of the National Transportation Safety Board.

16

towards the Mount Royal portal. The properties of the brick were assumed as follows: thermal conductivity 0.7 W/(m·K), specific heat 835 J/(kg·K), density 1,920 kg/m^3 [11]. There is a range of thermal properties for brick. The values cited here are in the middle of the range. The effects of varying the properties will be discussed in Section 6. Because of the long burn time of the Howard Street Tunnel fire, the simulations were carried out for as long as it was necessary to achieve a relatively constant wall surface temperature. Once all of the solid surfaces within the tunnel (tunnel wall, train car steel walls) heated up to steady-state, it was assumed that the gas temperature would also remain steady.

There is a fair amount of uncertainty as to how large a spill area was created following the rupture of the tank car carrying the tripropylene. It was reported by the NTSB that the tripropylene spilled from a 1.5 inch (4 cm) hole near the bottom of the cylindrical tank [1]. The initial flow from the hole was estimated via the relation

$$\dot{V} = C A \sqrt{\frac{2 \, \Delta P}{\rho}} \qquad (2)$$

where C is an orifice coefficient, equal to about 0.7, A is the area of the hole, ΔP is essentially the pressure near the bottom of tank, and ρ is the density of the liquid. From this relation, it was estimated that the fuel initially spilled at a rate of approximately 1,000 L/min (250 gal/min). The rate decreased over time as the pressure at the hole decreased, although it is possible that the heat from the fire could have slowed the rate at which the pressure decreased by heating up the air within the tank. In any event, we can conservatively bracket the time required for the car to empty its contents from two to four hours.

The heat of combustion of tripropylene is about 44,300 kW/kg; its density is 0.74 kg/L. If the spilling fuel were to have burned immediately upon its release without forming a pool, the heat release rate of the fire would have been about 1,000 MW. Rough calculations were performed initially that indicated that a fire of this size could not have been sustained in the tunnel due to the lack of sufficient oxygen to consume the fuel. Thus, it was assumed that the spilling tripropylene soaked into the roughly 1 ft (30 cm) layer of ballast (fist-sized rocks) between and below the ties of the railroad tracks.

Burning rates of liquid fuels are typically measured in deep obstruction-free pools. Because both the area and burning rate of the fuel-soaked ballast are subject to considerable uncertainty, a range of burn areas and rates had to be considered in the study. As a first estimate, the burn area was assumed to have been 12 m^2 (130 ft^2). The burn area was increased from this size to determine the sensitivity of the tunnel temperatures to the size of the pool. The car carrying the tripropylene held approximately 110,000 L (28,700 gal). The time required to burn this much fuel is proportional to the burn area. Based on measurements of similar liquid hydrocarbon fuels burning in deep pools under fully-ventilated conditions [10], the peak burning rate of the tripropylene (nonene) per unit area was estimated to have been 0.06 kg/(m^2·s) or 0.08 L/(m^2·s) (7 gal/(ft^2·h)). Although the tripropylene did not necessarily form a deep pool, the estimate was applied to the burning rate of fuel-soaked ballast. To simplify the analysis, rather than varying the area of the fuel bed and the burning rate per unit area, the burning rate was assumed constant and the area varied.

It is difficult to estimate how long the fire in the tunnel would have lasted for a number of reasons. First, some of the fuel could have drained through grates in the floor of the tunnel. Second, a considerable fraction of the fuel would have evaporated but not burned due to the high heat flux

17

to the fuel bed but low oxygen level in the tunnel. A tunnel fire is an example of a very inefficient combustion system. Unlike in an efficient commercial furnace, the large amount of fuel and small amount of oxygen lead to a substantial increase in the production of soot (black smoke), carbon monoxide, unburned fuel, and various other products of incomplete combustion.

Complicating the estimate of the burn time is the fact that at 6:19 pm, approximately three hours after the fire started, a water main crossing just below the tunnel ceiling and running perpendicular to the tunnel at Lombard Street, ruptured, and water poured into the tunnel. Estimates of the amount of water spilled vary, but it was substantial. It was observed by Baltimore City Fire Department (BCFD) officials that water filled the intersection of Howard and Lombard Streets to a depth of about 1 ft (30 cm). The water had a significant effect on the fire below because at 6:58 pm, 39 min after the pipe ruptured, BCFD officials commented that there was a noticeable change in the color of the smoke pouring from the Mount Royal portal, from dark black to gray. Preliminary calculations showed that the velocity of the smoke and hot gases near the ceiling of the tunnel flowing towards the Mount Royal portal was on the order of 1 m/s (3 ft/s, 2 mi/h). At this rate, it would have taken on the order of 30 min for the smoke to have traversed the 1,900 m (6,300 ft) between Lombard Street and Mount Royal. Because some time would have been required for the water to affect the fire, plus a weaker fire would not have driven the smoke as quickly, the appearance of whiter smoke approximately 40 min after the pipe rupture can be attributed directly to the introduction of a substantial amount of water into the tunnel near the fire.

It is not known to what extent the water reduced the size of the fire. NTSB interviews indicate that when fire fighters were able to approach the tripropylene car twelve hours after the fire started, it was not burning. It can thus be assumed that the fire burned at full strength for three hours, potentially burned for several more hours but at a reduced rate due to the introduction of water, and exhausted itself either due to a lack of fuel or extinguishment by water after twelve hours. Smoldering fires continued in the closed box cars for several days during which time emergency responders pulled the cars from the tunnel.

The calculations to be discussed next simulate the first half hour of the fire. The predicted gas and surface temperatures reach a steady-state in this amount of time, allowing for an assessment of the thermal environment for the time period before the water main break.

5   Calculation Results

Shown in Fig. 10 are vertical centerline temperature contours at two stages during the simulated fire in the Howard Street Tunnel. Initially, the fire would have been well-ventilated; that is, it would have had access to a supply of oxygen comparable to the outside. However, as the tunnel filled with smoke and other combustion products, the fire would have become oxygen-limited, especially on the up-slope side of the fire. Since the air movement in the tunnel would have been biased towards the uphill portal (Mount Royal Station), one would expect to see the fire pushed over towards the right in the figures. This effect was more pronounced in the Memorial Tunnel experiment, where the air flow through the tunnel was uni-directional uphill. The Howard Street Tunnel is about one-fourth as steep as the Memorial Tunnel, and smoke was observed pouring from both portals. The uphill side of the fire shows slightly lower oxygen concentrations, as seen in Fig. 11.

The segment of the tunnel shown is a small fraction of the overall length. The entire tunnel volume was included in the calculation so that the mixing of fresh air and hot smoke along the entire tunnel length could be simulated. The mixing process dictates where the boundary between the hot upper layer and cooler lower layer will be located. This is an important finding because train cars that were pulled from the tunnel a few days after the initial derailment show discoloration above a height of a few meters. The level at which the discoloration begins varies, depending on how far from the fire the car was. Photos of some tank cars show damage roughly two-thirds of the way up the height of the car, while some box cars show damage starting about one-third of the way up. See Figs. 13 – 15.

The extent of the damage to objects within the tunnel is a function of the gas temperature surrounding the object and the radiative heat flux to the object from nearby hot objects or fire. Typically, objects closer to the ground are subjected to less direct heating from hot gases, but they do absorb radiant energy from the hotter gas layer above. For the simulations of the Howard Street Tunnel fire, the temperature and heat flux was estimated at the tunnel ceiling and floor, to bracket the range of temperature and heat flux to which objects in the tunnel may have been exposed. The estimates indicate that surfaces that were exposed to direct flame impingement were subjected to heat fluxes in a range from 100 kW/m^2 to 150 kW/m^2. These surfaces would include the tunnel ceiling above the fire, and the sides of the rail cars directly within the fire. This magnitude of heat flux has been measured at Sandia National Laboratories in fire experiments involving large objects suspended in large, open hydrocarbon pool fires [12]. Surfaces that were exposed to the hot, smoke-laden gases flowing near the tunnel ceiling, like the tops of the rail cars, are estimated to have seen heat fluxes in the range of 40 kW/m^2 to 80 kW/m^2, depending on the proximity to the fire. Ultimately, the steel rail cars heated up to a temperature very near the gas temperature. After the tripropylene had been consumed, the closed rail cars containing smoldering paper products probably maintained a temperature on the order of 300 °C (570 °F), consistent with the temperature at which paper undergoes thermal degradation into pyrolyzates. The basis of this speculation is the fact that several cars burst into flames when they were opened up in the course of extinguishing the smoldering materials inside. The introduction of oxygen to the closed cars caused the transition from smoldering to flaming combustion.

FIGURE 10: Predicted temperatures along the centerline vertical plane at 5 and 30 min after ignition of the Howard Street Tunnel fire. The region shown encompasses the rail cars nearest the tripropylene spill. The temperatures decrease in the tunnel as the fire becomes oxygen-limited. The white rectangular boxes in each frame represent rail cars through which the temperature slice cuts. The tunnel slopes upwards from left to right.
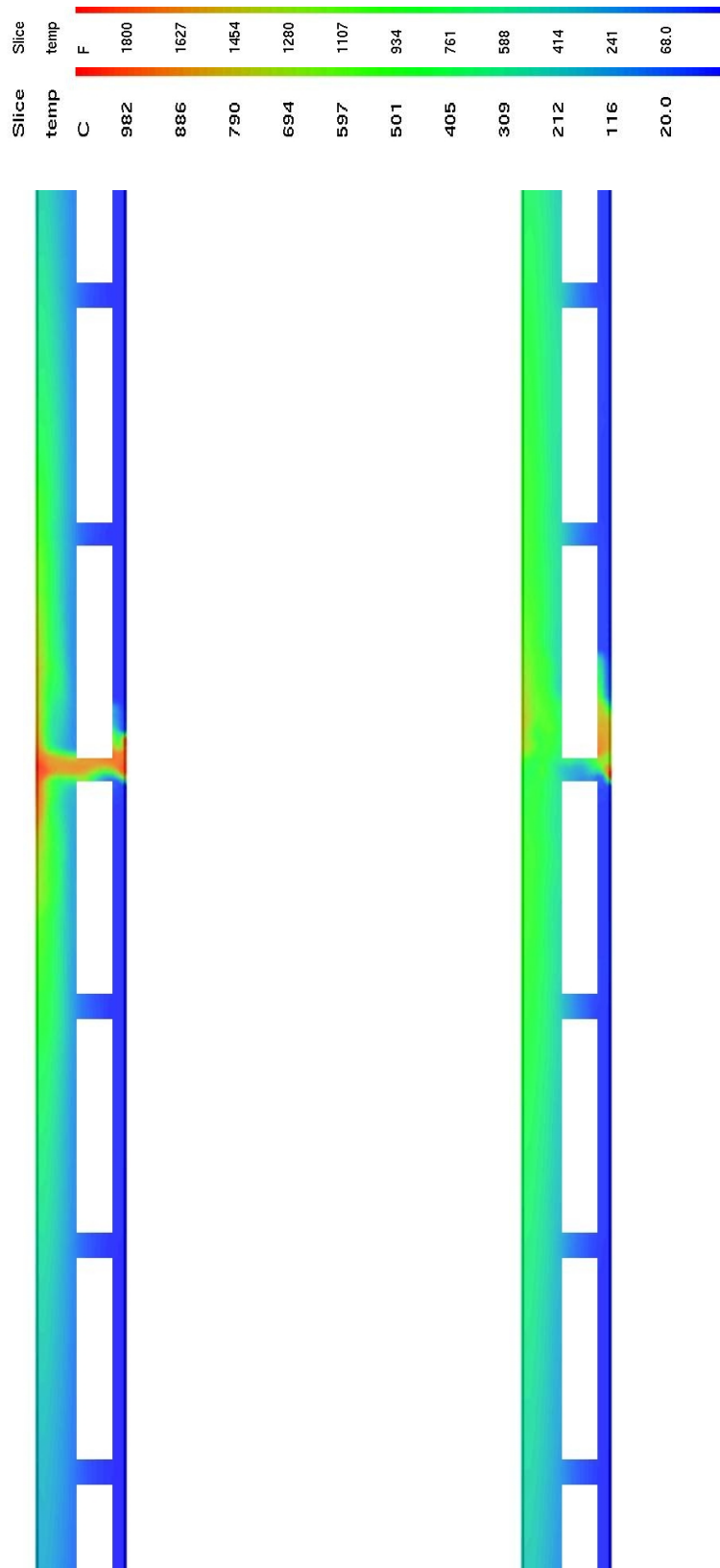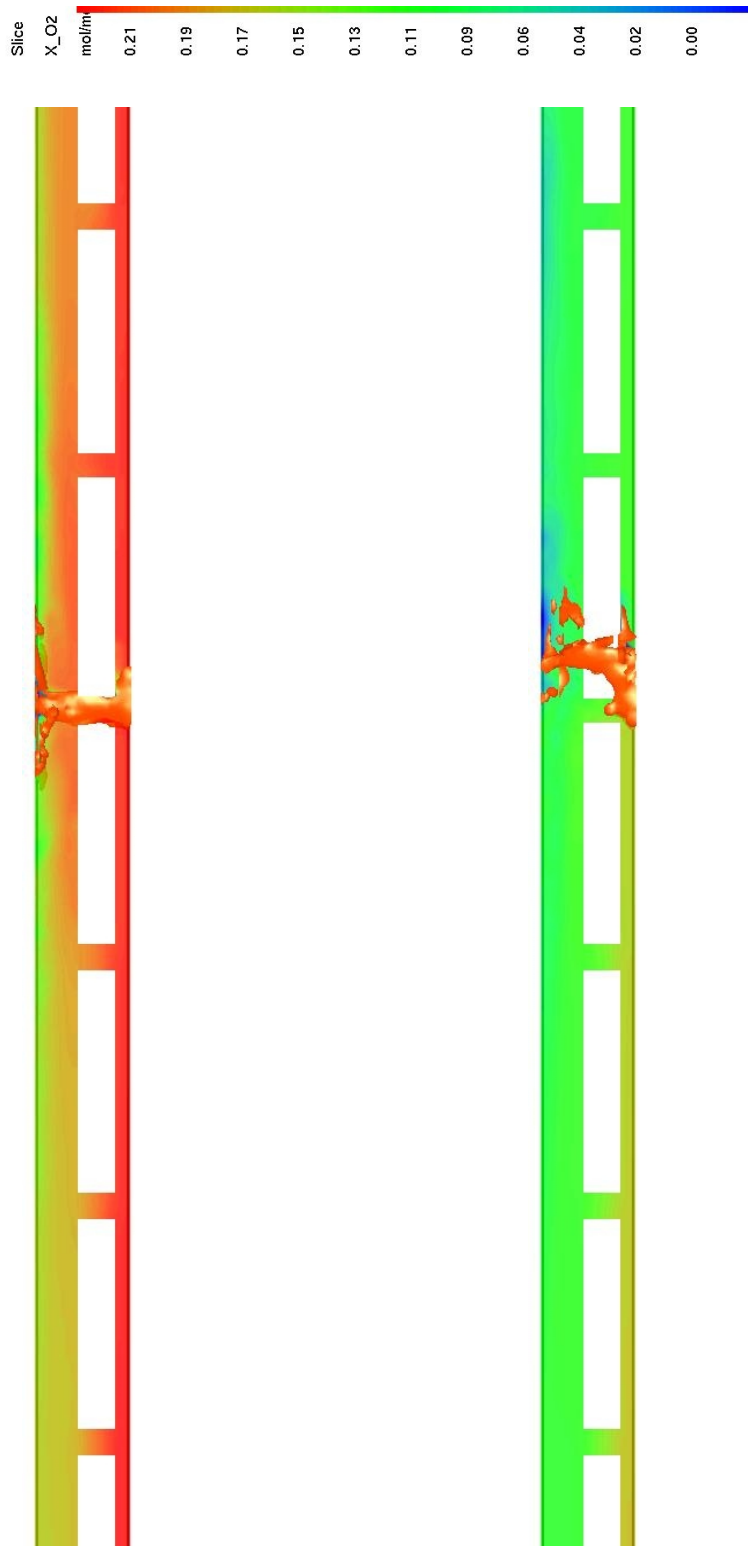
FIGURE 11: Predicted oxygen concentration along the centerline vertical plane at 5 and 30 min after ignition of the Howard Street Tunnel fire. The region shown encompasses the rail cars nearest the tripropylene spill. The flaming region is shown in orange. The white rectangular boxes in each frame represent the outline of the rail cars. The tunnel slopes upwards from left to right.
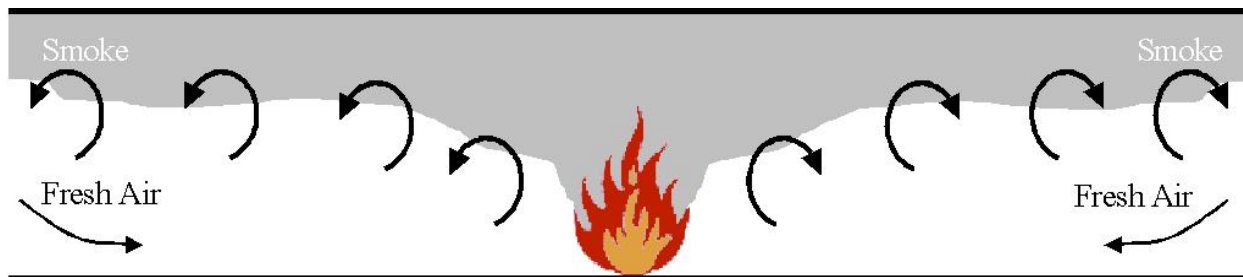
FIGURE 12: Schematic diagram showing how smoke and fresh air mix within a tunnel.

6 Analysis and Discussion

In this section, we will analyze the results of the calculations presented, and consider the uncertainty of the results by varying the most sensitive input parameters to the model. The first question to consider is how fast was the tripropylene consumed; next, what were the temperatures of the brick walls and steel rail cars; and finally, how would these findings change if the input parameters were varied. This is how most fire analysis is done – how much energy is produced, and where does this energy go?

6.1 Burning Rate

A fire requires fuel, oxygen and a source of heat to sustain itself. In a confined space, it is usually oxygen that is in short supply, thus the name given to these types of fires is "oxygen-limited." The size of the Howard Street Tunnel fire appears to have been limited to about 50 MW based on the various calculations that were performed.[3] In some calculations, only the pool area was specified, and the fuel was allowed to evaporate based on the thermal heat flux impinging on the fuel surface. In others, a fixed heat release rate was used based on the estimated size of the pool and the properties of the fuel. In both cases, the heat release rate was about 50 MW. Often more fuel vaporizes than is actually burned in oxygen-limited fires, and even the fuel that is consumed is not burned efficiently, hence the black smoke.

From the estimated heat release rate of the fire, we can estimate the amount of oxygen (and air) that reached the fire from outside the tunnel. Figure 12 is a schematic diagram showing how smoke and fresh air mix along the interface between the hot upper layer of smoke and cool lower layer of fresh air. Given that the tunnel is 2.65 km (1.65 mi) in length, much of the fresh air that entered the tunnel during the fire was mixed with the exiting smoke and never reached the fire. Given that most hydrocarbon fires (including tripropylene) consume oxygen at a rate of 13,000 kJ/kg, a 50,000 kW fire would consume oxygen at a rate of about 4 kg/s. The volume of air required to provide this amount of oxygen is about 14 m^3/s (30,000 cfm). Because most of the air reaching the fire would have had to come from the Camden and Mount Royal portals, the fire could not have burned fuel at a greater rate than it did because of oxygen limitations.

---

[3]To put this number in perspective, 50 MW (or 50,000 kW) is roughly the heat release rate of a small single family house engulfed in flames.

22

FIGURE 13: Box car from the Howard Street Tunnel. Photo courtesy of the National Transportation Safety Board.

FIGURE 14: Tripropylene tank car (#52) after the fire, shown from the left side. The fuel spilled out of hole near the bottom of the tank at the right. The car in front is a box car carrying paper (car #51 out of 60). Courtesy Nancy McAtee of the National Transportation Safety Board.

FIGURE 15: Right side of car #53, a tank car carrying hydrochloric acid. Courtesy Nancy McAtee of the National Transportation Safety Board.

6.2   Parameter Study

Throughout the course of the investigation into the thermal environment of the Howard Street Tunnel fire, several dozen simulations were performed based on descriptions of the train, the tunnel, and the fuel spill. An examination of photographs taken by the NTSB during and after the incident helped to narrow down the range of potential fire scenarios. The calculations showed small variations in results, but nothing that would significantly affect the overall conclusions.

The most important quantity in any fire analysis is the heat release rate of the fire. In fact, the focus of fire modeling is to predict how the energy from the fire is distributed throughout the volume of interest. As was discussed above, the fire in the Howard Street Tunnel was most likely oxygen-limited, that is, the heat release rate of the fire was constrained by the supply of oxygen, not fuel, which is usually the case with large fires in enclosures. In the calculations, the size of the pool of liquid fuel was varied, the parameters governing the evaporation process were varied, and various fixed fuel evaporation rates were prescribed. In all cases, the heat release rate of the fire was about 50 MW or less. The unburned fuel gases were mixed in with the exhaust gases and vented out the tunnel exits without having burned.

Given that the peak heat release rate of the fire was about 50 MW, the next issue to consider is how much of that energy was absorbed by the tunnel walls, and how much was lost to the atmosphere via the black smoke. Given the length of the tunnel, most of the fire's heat was absorbed by the walls. The temperature of the smoke exiting the tunnel at both ends was very nearly ambient, based on the results of the calculations. Since the tunnel walls were absorbing the heat, the thermal properties of the brick was an important consideration. Various sources in the heat transfer and fire literature [11, 13] report the thermal conductivity of brick to range between 0.5 W/(m·K) to 1.0 W/(m·K), the density 1,500 kg/m^3 to 3,000 kg/m^3, the specific heat 800 J/(kg·K) to 1000 J/(kg·K). Because the brick used in the Howard Street Tunnel is difficult to characterize, calculations were performed using a range of thermal properties for the brick walls to determine what effect this would have on the final temperatures within the tunnel. The baseline calculation was run with a thermal conductivity of 0.7 W/(m·K). Calculations with values of 0.45 W/(m·K) and 1.0 W/(m·K) were run to check the sensitivity of the results. The peak surface temperature at the ceiling for the baseline case was approximately 700 °C (1,300 °F), whereas when the lower value of the thermal conductivity was used, the peak temperature was approximately 800 °C (1,500 °F). When the higher value of conductivity was used, the peak temperature was approximately 600 °C (1,100 °F). It is expected that a more conductive wall lining would be less hot than a more insulating lining because the more conductive lining conducts heat away at a greater rate. Note that these temperatures are being rounded off to the nearest hundred degrees Celsius to indicate that the location of the hottest point on the tunnel ceiling shifts with the fire. These temperatures were predicted where flames were simulated to have impinged on the ceiling. The intent of this study is to gauge the sensitivity of the simulation results to the input parameters.

One additional sensitivity study was performed simply as a result of varying the geometry of the tunnel and train cars contained within the tunnel as more detailed information was made available. The original simulations of the fire were performed under the assumption that the tunnel was nominally 6.1 m (20 ft) high and 9.1 m (30 ft) wide. The cars were assumed to be solid blocks 3.0 m (10 ft) wide and 4.0 m (13 ft) high with 1.0 m (3 ft) of void space beneath to represent the undercarriage. Most of the cars were centered in the tunnel, but several of the derailed cars were offset based on the diagram of the accident scene provided by the NTSB. The cars in the simulation

served as targets of thermal radiation and obstructions limiting the airflow to the fire. Specific damage to the cars was not included in the simulations. Throughout the study, the car dimensions remained the same, but the tunnel dimensions were varied based on information provided by the NTSB. In the vicinity of the fire, the actual dimensions of the tunnel are 9.9 m (32.5 ft) wide by 6.4 m (21.0 ft) high. The section of the tunnel north of the accident is approximately 8.2 m (27 ft) wide by 6.7 m (22 ft) high. Because of resolution limits of the numerical grid, the width of 8.2 m (27 ft) and a height of 7.3 m (24 ft) was used for most of the simulations. It was found that the variations in tunnel width and height had no measurable effect on the results of the study.

7 Conclusion

The Howard Street Tunnel fire in Baltimore in July, 2001, has been modeled using the Fire Dynamics Simulator, a computational fluid dynamics fire model developed by the National Institute of Standards and Technology. The objective of the calculations has been to quantify the peak gas and surface temperatures that were likely reached during a several hour period in which a pool of spilled tripropylene burned. As a validation of the numerical model, several fire tests conducted in a decommissioned highway tunnel in West Virginia were simulated, with peak temperatures between experiment and model agreeing within about 50 °C (90 °F).

The simulations of the Howard Street Tunnel fire address the behavior of the fire from its ignition until the rupture of a water main three hours later. The simulations suggest that during this time period the fire was oxygen-limited, that is, the heat release rate of the fire was limited to about 50 MW by the amount of oxygen that could reach the fire. During this time, some of the spilled tripropylene evaporated but could not burn for lack of oxygen, and some drained off through grates in the tunnel floor. The exact distribution of the fuel is hard to predict, thus predicting the duration of the fire, with or without the rupturing of the water main, would be difficult. Between three and twelve hours after ignition, the tripropylene fire self-extinguished either due to a lack of fuel or suppression by water. Beyond twelve hours, the combustible products within the closed box cars continued to smolder for several days, but at temperatures far less than those experienced during the flaming combustion of the liquid fuel.

The peak calculated temperatures within the tunnel during the first three hours (before the water main rupture) were approximately 1,000 °C (1,800 °F) within the flaming regions or about half of the length of a rail car, and approximately 500 °C (900 °F) when averaged over a length of the tunnel equal to the length of three to four rail cars. Because of the insulation provided by the thick brick walls of the tunnel, the temperatures within a few car lengths of the fire were relatively uniform, consistent with what one would expect to find in an oven or furnace. According to the calculations, the peak calculated wall surface temperature reached about 800 °C (1,500 °F) where the flames were directly impinging, and 400 °C (750 °F) over the length of three to four rail cars. The steel temperature of the rail cars would be expected to be similar to the surrounding gas temperature because of the long exposure time and high thermal conductivity of steel.

A sensitivity study was undertaken to ensure that variations in the physical parameters of the model and the accident scenario would not lead to dramatic changes in the overall results. The fact that the fire within the tunnel would have very soon become oxygen-limited reduced the possibility for wide variations in the outcome of the study.

References

[1] NTSB Fire Group – Factual Report. NTSB Public Docket, Report Issue Date: October 2002. NTSB Case Reference Number: DCA 01 MR 004; Accident Site Location Reference: Baltimore, MD (Howard Street Tunnel); Accident Date Reference: July 18, 2001.

[2] K.B. McGrattan, H.R. Baum, R.G. Rehm, G.P. Forney, J.E. Floyd, and S. Hostikka. Fire Dynamics Simulator (Version 2), Technical Reference Guide. Technical Report NISTIR 6783, National Institute of Standards and Technology, Gaithersburg, Maryland, November 2001.

[3] K.B. McGrattan, G.P. Forney, J.E. Floyd, and S. Hostikka. Fire Dynamics Simulator (Version 2), User's Guide. Technical Report NISTIR 6784, National Institute of Standards and Technology, Gaithersburg, Maryland, November 2001.

[4] S. Hostikka, H.R. Baum, and K.B. McGrattan. Large Eddy Simulations of the Cone Calorimeter. In *Proceedings of US Section Meeting of the Combustion Institute, Oakland, California*, March 2001.

[5] K.B. McGrattan, H.R. Baum, and R.G. Rehm. Large Eddy Simulations of Smoke Movement. *Fire Safety Journal*, 30:161–178, 1998.

[6] K.B. McGrattan, A. Hamins, and D. Stroup. Sprinkler, Smoke & Heat Vent, Draft Curtain Interaction — Large Scale Experiments and Model Development. Technical Report NISTIR 6196-1, National Institute of Standards and Technology, Gaithersburg, Maryland, September 1998.

[7] International Collaborative Project to Evaluate Fire Models for Nuclear Power Plant Applications – Summary of Planning Meeting. Technical Report NUREG/CP-0170, Nuclear Regulatory Commission, 2000.

[8] Memorial Tunnel Fire Ventilation Test Program. Test Report, Massachusetts Highway Department, 1995.

[9] J. Quintiere. A Perspective on Compartment Fire Growth. *Combustion Science and Technology*, 39:11–54, 1984.

[10] V. Babrauskas. *SFPE Handbook*, chapter Burning Rates. National Fire Protection Association, Quincy, Massachusetts, 2nd edition, 1995.

[11] F.P. Incropera and D.P. De Witt. *Fundamentals of Heat and Mass Transfer*. John Wiley and Sons, New York, 3rd edition, 1990.

[12] M.A. Kramer, M. Greiner, and J.A. Koski. Radiation Heat Transfer to the Leeward Side of a Massive Object Suspended over a Pool Fire. In *Proceedings of 2001 ASME International Mechanical Engineering Congress and Exposition*. American Society of Mechanical Engineering, November 2001. IMECE2001/HTD-24250.

[13] J.G. Quintiere. *Principles of Fire Behavior*. Delmar Publishers, Albany, New York, 1998.

[14] R.G. Rehm and H.R. Baum. The Equations of Motion for Thermally Driven, Buoyant Flows. *Journal of Research of the NBS*, 83:297–308, 1978.

[15] H.R. Baum and K.B. McGrattan. Simulation of Large Industrial Outdoor Fires. In *Fire Safety Science – Proceedings of the Sixth International Symposium*. International Association for Fire Safety Science, 1999.

[16] C. Huggett. Estimation of the Rate of Heat Release by Means of Oxygen Consumption Measurements. *Fire and Materials*, 4:61–65, 1980.

[17] W. Grosshandler. RadCal: A Narrow Band Model for Radiation Calculations in a Combustion Environment. NIST Technical Note (TN 1402), National Institute of Standards and Technology, Gaithersburg, Maryland 20899, 1993.

[18] G.D. Raithby and E.H. Chui. A Finite-Volume Method for Predicting Radiant Heat Transfer in Enclosures with Participating Media. *Journal of Heat Transfer*, 112(2):415–423, 1990.

[19] J.P. Holman. *Heat Transfer*. McGraw-Hill, New York, 5th edition, 1989.

[20] K. Prasad, C. Li, K. Kailasanath, C. Ndubizu, R. Ananth, and P.A. Tatem. Numerical modelling of methanol liquid pool fires. *Combustion Theory and Modelling*, 3:743–768, 1999.

A   Numerical Method

The Fire Dynamics Simulator (FDS) is publicly available software maintained by the National Institute of Standards and Technology (NIST). It can be downloaded from the web site

`http://fire.nist.gov/fds`

The numerical method used in FDS is documented in Reference [2], and instructions on how to use the model are given in Reference [3]. As of the publication of this report, the released version of FDS is 2.0. Some of the physical mechanisms discussed below needed for this project will be available in the next release of FDS.

A.1   Conservation Equations

An approximate form of the Navier-Stokes equations appropriate for low Mach number applications is used in the model. The approximation involves the filtering out of acoustic waves while allowing for large variations in temperature and density [14]. This gives the equations an elliptic character, consistent with low speed, thermal convective processes. To handle sub-grid scale convective motion, a large eddy simulation (LES) technique is used in which the large-scale eddies are computed directly and the sub-grid scale dissipative processes are modeled.

Consider the conservation equations of mass, momentum and energy for a thermally-expandable, multi-component mixture of ideal gases [14]:

Conservation of Mass

$$\frac{\partial \rho}{\partial t} + \nabla \cdot \rho \mathbf{u} = 0 \tag{3}$$

Conservation of Species

$$\frac{\partial}{\partial t}(\rho Y_l) + \nabla \cdot \rho Y_l \mathbf{u} = \nabla \cdot (\rho D)_l \nabla Y_l + \dot{W}_l''' \tag{4}$$

Conservation of Momentum

$$\rho \left(\frac{\partial \mathbf{u}}{\partial t} + (\mathbf{u} \cdot \nabla)\mathbf{u} \right) + \nabla p = \rho \mathbf{g} + \nabla \cdot \tau \tag{5}$$

Conservation of Energy

$$\frac{\partial}{\partial t}(\rho h) + \nabla \cdot \rho h \mathbf{u} - \frac{Dp}{Dt} = \dot{q}''' - \nabla \cdot \mathbf{q}_r + \nabla \cdot k \nabla T + \nabla \cdot \sum_l h_l (\rho D)_l \nabla Y_l \tag{6}$$

The symbols have their usual meanings: ρ is the density, $\mathbf{u}$ is the velocity vector, Y_l is the mass fraction of species l, $\dot{W}_l'''$ is the mass production rate of species l per unit volume, p is the pressure, $\mathbf{g}$ is the gravity vector, τ is the viscous stress tensor, h is the enthalpy, $\dot{q}'''$ is the heat release rate per unit volume, $\mathbf{q}_r$ is the radiative flux, T is the temperature, k is the thermal conductivity, and D is the material diffusivity. The energy driving the system is represented by the heat release rate $\dot{q}'''$ in Eq. (6). The term $Dp/Dt = \partial p/\partial t + \mathbf{u} \cdot \nabla p$ is a material derivative.

The conservation equations are supplemented by an equation of state relating the thermodynamic quantities density, pressure and enthalpy; ρ, p and h. The pressure is decomposed into three components

$$p = p_0 - \rho_\infty gz + \tilde{p} \tag{7}$$

The first term on the right hand side is the "background" pressure, the second is the hydrostatic contribution, and the third is the flow-induced perturbation pressure. For most applications, p_0 is constant. However, if the enclosure is tightly sealed, p_0 is allowed to increase (or decrease) with time as the pressure within the enclosure rises due to thermal expansion or falls due to forced ventilation. Also, if the height of the domain is on the order of a kilometer, p_0 can no longer be assumed constant and must be considered a function of the altitude [15].

The purpose of decomposing the pressure is that for low-Mach number flows, it can be assumed that the temperature and density are inversely proportional, and thus the equation of state can be approximated [14]

$$p_0 = \rho T \mathcal{R} \sum (Y_i/M_i) = \rho T \mathcal{R}/M \tag{8}$$

The pressure p in the state and energy equations is replaced by the background pressure p_0 to filter out sound waves that travel at speeds that are much faster than typical flow speeds expected in fire applications. The low Mach number assumption serves two purposes. First, the filtering of acoustic waves means that the time step in the numerical algorithm is bound only by the flow speed as opposed to the speed of sound, and second, the modified state equation leads to a reduction in the number of dependent variables in the system of equations by one. The energy equation (6) is never explicitly solved, but its source terms are included in the expression for the flow divergence, an important quantity in the analysis to follow.
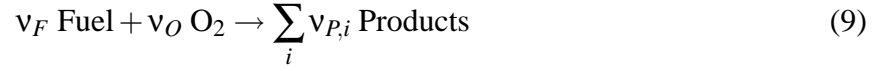
A.2 Combustion

The mixture fraction combustion model is based on the assumption that large-scale convective and radiative transport phenomena can be simulated directly, but physical processes occurring at small length and time scales must be represented in an approximate manner. The nature of the approximations employed are necessarily a function of the spatial and temporal resolution limits of the computation, as well as our current (often limited) understanding of the phenomena involved.

The actual chemical rate processes that control the combustion energy release are often unknown in fire scenarios. Even if they were known, the spatial and temporal resolution limits imposed by both present and foreseeable computer resources places a detailed description of combustion processes beyond reach. Thus, the model adopted here is based on the assumption that the combustion is mixing-controlled. This implies that all species of interest can be described in terms of a mixture fraction $Z(\mathbf{x},t)$. The mixture fraction is a conserved quantity representing the fraction of material at a given point that originated as fuel. The relations between the mass fraction of each species and the mixture fraction are known as "state relations". The state relation for the oxygen mass fraction provides the information needed to calculate the local oxygen mass consumption rate. The form of the state relation that emerges from classical laminar diffusion flame theory is a piecewise linear function. This leads to a "flame sheet" model, where the flame is a two dimensional surface embedded in a three dimensional space. The local heat release rate is computed from the local oxygen consumption rate at the flame surface, assuming that the heat release rate

is directly proportional to the oxygen consumption rate, independent of the fuel involved. This relation, originally proposed by Huggett [16], is the basis of oxygen calorimetry.

Start with the most general form of the combustion reaction

$$\nu_F \text{ Fuel} + \nu_O \text{ O}_2 \rightarrow \sum_i \nu_{P,i} \text{ Products} \tag{9}$$

The numbers ν_i are the stoichiometric coefficients for the overall combustion process that reacts fuel "F" with oxygen "O" to produce a number of products "P". The stoichiometric equation (9) implies that the mass consumption rates for fuel and oxidizer are related as follows:

$$\frac{\dot{m}_F'''}{\nu_F M_F} = \frac{\dot{m}_O'''}{\nu_O M_O} \tag{10}$$

The mixture fraction Z is defined as:

$$Z = \frac{s Y_F - (Y_O - Y_O^\infty)}{s Y_F^I + Y_O^\infty} \quad ; \quad s = \frac{\nu_O M_O}{\nu_F M_F} \tag{11}$$

By design, it varies from $Z = 1$ in a region containing only fuel to $Z = 0$ where the oxygen mass fraction takes on its undepleted ambient value, Y_O^∞. Note that Y_F^I is the fraction of fuel in the fuel stream. The quantities M_F and M_O are the fuel and oxygen relative molecular masses, respectively. The mixture fraction satisfies the conservation law

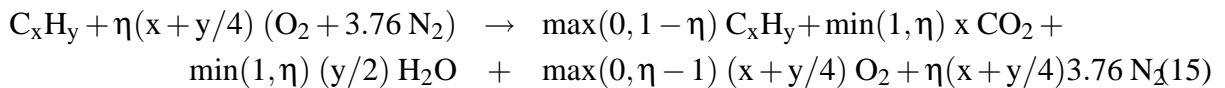$$\rho \frac{DZ}{Dt} = \nabla \cdot \rho D \nabla Z \tag{12}$$

obtained from a linear combination of the fuel and oxygen conservation equations. The assumption that the chemistry is "fast" means that the reactions that consume fuel and oxidizer occur so rapidly that the fuel and oxidizer cannot co-exist. The requirement that fuel and oxidizer simultaneously vanish defines a flame surface as:

$$Z(\mathbf{x}, t) = Z_f \quad ; \quad Z_f = \frac{Y_O^\infty}{s Y_F^I + Y_O^\infty} \tag{13}$$

The assumption that fuel and oxidizer cannot co-exist leads to the "state relation" between the oxygen mass fraction Y_O and Z

$$Y_O(Z) = \begin{cases} Y_O^\infty (1 - Z/Z_f) & Z < Z_f \\ 0 & Z > Z_f \end{cases} \tag{14}$$

State relations for both reactants and products can be derived by considering the following ideal reaction of a hydrocarbon fuel:

$$\begin{aligned} \text{C}_x\text{H}_y + \eta(x + y/4)\,(\text{O}_2 + 3.76\,\text{N}_2) \quad &\rightarrow \quad \max(0, 1 - \eta)\,\text{C}_x\text{H}_y + \min(1, \eta)\,x\,\text{CO}_2 + \\ \min(1, \eta)\,(y/2)\,\text{H}_2\text{O} \quad &+ \quad \max(0, \eta - 1)\,(x + y/4)\,\text{O}_2 + \eta(x + y/4)3.76\,\text{N}_2 \end{aligned} \tag{15}$$

Here η is a parameter ranging from 0 (all fuel with no oxygen) to infinity (all oxygen with no fuel). A correspondence between η and Z is obtained by applying the definition of Z (Eq. 11) to the left hand side of Eq. (15). Mass fractions of the products of the infinitely fast reaction (including
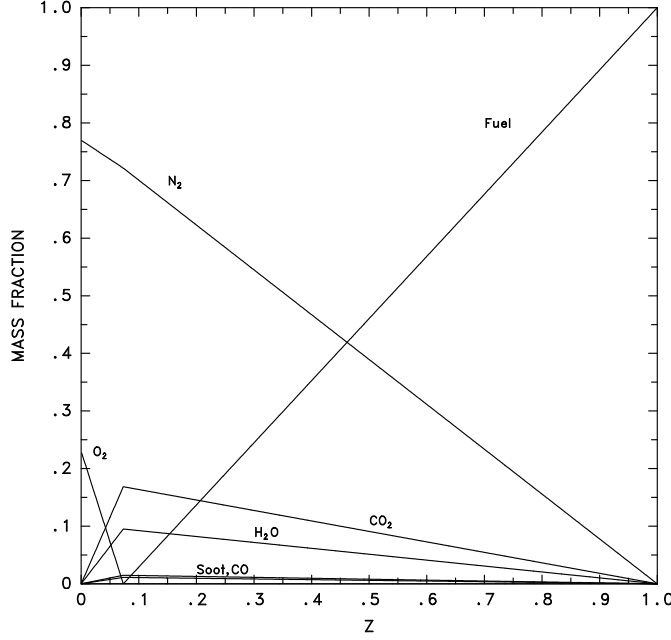
FIGURE 16: State relations for nonene. The soot yield is assumed to be 0.15 and the CO yield is assumed to be 0.20, where the yield is the mass of product produced per mass of fuel burned.

excess fuel or oxygen) can be obtained from the right hand side of Eq. (15). State relations for the ideal reaction of nonene and air is shown in Fig. 16.

An expression for the local heat release rate can be derived from the conservation equations and the state relation for oxygen. The starting point is Huggett's [16] relationship for the heat release rate as a function of the oxygen consumption

$$\dot{q}''' = \Delta H_O \dot{m}_O''' \tag{16}$$

Here, ΔH_O is the heat release rate per unit mass of oxygen consumed. The oxygen mass conservation equation

$$\rho \frac{DY_O}{Dt} = \nabla \cdot \rho D \nabla Y_O + \dot{m}_O''' \tag{17}$$

can be transformed into an expression for the local heat release rate using the conservation equation for the mixture fraction (12) and the state relation for oxygen $Y_O(Z)$.

$$-\dot{m}_O''' = \nabla \cdot \left(\rho D \frac{dY_O}{dZ} \nabla Z \right) - \frac{dY_O}{dZ} \nabla \cdot \rho D \nabla Z = \rho D \frac{d^2 Y_O}{dZ^2} |\nabla Z|^2 \tag{18}$$

Neither of these expressions for the local oxygen consumption rate is particularly convenient to apply numerically because of the discontinuity of the derivative of $Y_O(Z)$ at $Z = Z_f$. However, an expression for the oxygen consumption rate per unit area of flame sheet can be derived from Eq. (18)

$$-\dot{m}_O'' = \left. \frac{dY_O}{dZ} \right|_{Z < Z_f} \rho D \, \nabla Z \cdot \mathbf{n} \tag{19}$$

34

In the numerical algorithm, the local heat release rate is computed by first locating the flame sheet, then computing the local heat release rate per unit area, and finally distributing this energy to the grid cells cut by the flame sheet. In this way, the ideal, infinitely thin flame sheet is smeared out over the width of a grid cell, consistent with all other gas phase quantities.

A.3 Thermal Radiation

The Radiative Transport Equation (RTE) for a non-scattering gas is

$$\mathbf{s} \cdot \nabla I_\lambda(\mathbf{x}, \mathbf{s}) = \kappa(\mathbf{x}, \lambda) \ [I_b(\mathbf{x}) - I(\mathbf{x}, \mathbf{s})] \tag{20}$$

where $I_\lambda(\mathbf{x}, \mathbf{s})$ is the radiation intensity at wavelength λ, $I_b(\mathbf{x})$ is the source term given by the Planck function, $\mathbf{s}$ is the unit normal direction vector and $\kappa(\mathbf{x})$ is the absorption coefficient. The source term can be written as a fraction of the blackbody radiation

$$I_b = \sigma \, T^4 / \pi \tag{21}$$

where σ is the Stefan-Boltzmann constant. In most large-scale fire scenarios soot is the most important combustion product controlling the thermal radiation from the fire and hot smoke. As the radiation spectrum of soot is continuous, it is possible to assume that the gas behaves as a gray medium. The spectral dependence is lumped into one absorption coefficient. For the calculation of the gray gas absorption coefficient, κ, a narrow-band model, RADCAL [17], has been implemented in FDS. At the start of a simulation the absorption coefficient is tabulated as a function of mixture fraction and temperature. During the simulation the local absorption coefficient is found by table-lookup.

The boundary condition for the radiation intensity leaving a gray diffuse wall is given as

$$I_w(\mathbf{s}) = \varepsilon I_{bw} + \frac{1 - \varepsilon}{\pi} \int_{\mathbf{s}' \cdot \mathbf{n}_w < 0} I_w(\mathbf{s}') \ |\mathbf{s}' \cdot \mathbf{n}_w| \ d\Omega \tag{22}$$

where $I_w(\mathbf{s})$ is the intensity at the wall, ε is the emissivity, and I_{bw} is the black body intensity at the wall.

The radiative transport equation (20) is solved using techniques similar to those for convective transport in finite volume methods for fluid flow [18], thus the name given to it is the Finite Volume Method (FVM). To obtain the discretized form of the RTE, the unit sphere is divided into a finite number of solid angles. In each grid cell a discretized equation is derived by integrating equation (20) over the cell ijk and the control angle $\delta\Omega^l$, to obtain

$$\int_{\Omega^l} \int_{V_{ijk}} \mathbf{s} \cdot \nabla I_n(\mathbf{x}, \mathbf{s}) dV d\Omega = \int_{\Omega^l} \int_{V_{ijk}} \kappa_n(\mathbf{x}) \ [I_{b,n}(\mathbf{x}) - I_n(\mathbf{x}, \mathbf{s})] \, dV d\Omega \tag{23}$$

The volume integral on the left hand side is replaced by a surface integral over the cell faces using the divergence theorem. Assuming that the radiation intensity $I(\mathbf{x}, \mathbf{s})$ is constant on each of the cell faces, the surface integral can be approximated by a sum over the cell faces.

The radiant heat flux vector $\mathbf{q}_r$ is defined

$$\mathbf{q}_r(\mathbf{x}) = \int \mathbf{s} I(\mathbf{x}, \mathbf{s}) \, d\Omega \tag{24}$$

The radiative loss term in the energy equation is

$$-\nabla \cdot \mathbf{q}_r(\mathbf{x}) = \kappa(\mathbf{x}) \left[U(\mathbf{x}) - 4\pi I_b(\mathbf{x}) \right] \quad ; \quad U(\mathbf{x}) = \int_{4\pi} I(\mathbf{x}, \mathbf{s}) \, d\Omega \tag{25}$$

In words, the net radiant energy gained by a grid cell is the difference between that which is absorbed and that which is emitted.

A.4 Convective Heat Transfer to Walls

The heat flux to a solid surface consists of gains and losses from convection and radiation. The radiative flux at the surface is obtained from the boundary condition for the radiation equation, Eq. (22).

The convective heat flux to the surface is obtained from a combination of natural and forced convection correlations

$$\dot{q}_c'' = h \, \Delta T \quad \text{W/m}^2 \quad ; \quad h = \max \left[C \, |\Delta T|^{\frac{1}{3}} \quad , \quad \frac{k}{L} \, 0.037 \, \text{Re}^{\frac{4}{5}} \, \text{Pr}^{\frac{1}{3}} \right] \quad \text{W/(m}^2 \cdot \text{K)} \tag{26}$$

where ΔT is the difference between the wall and the gas temperature (taken at the center of the grid cell abutting the wall), C is the coefficient for natural convection (1.43 for a horizontal surface and 0.95 for a vertical surface) [19], L is a characteristic length related to the size of the physical obstruction, k is the thermal conductivity of the gas, and the Reynolds Re and Prandtl Pr numbers are based on the gas flowing past the obstruction. Since the Reynolds number is proportional to the characteristic length, L, the heat transfer coefficient is weakly related to L. For this reason, L is taken to be 1 m for most calculations.

If the surface material is assumed to be thermally-thick, a one-dimensional heat conduction equation for the material temperature, $T_s(x,t)$, is applied in the direction x pointing into the air/solid interface ($x = 0$)

$$\rho_s \, c_s \, \frac{\partial T_s}{\partial t} = k_s \, \frac{\partial^2 T_s}{\partial x^2} \quad ; \quad -k_s \frac{\partial T_s}{\partial x}(0,t) = \dot{q}_c'' + \dot{q}_r'' - \dot{m}'' \, \Delta H_v \tag{27}$$

where ρ_s, c_s and k_s are the (constant) density, specific heat and conductivity of the material; $\dot{q}_c''$ is the convective and $\dot{q}_r''$ is the (net) radiative heat flux at the surface, $\dot{m}''$ is the mass loss rate if burning is occurring, and ΔH_v is the heat of vaporization. It is assumed that fuel pyrolysis takes place at the surface; thus the heat required to vaporize fuel is extracted from the incoming energy flux.

The rate at which liquid fuel evaporates when burning is a function of the liquid temperature and the concentration of fuel vapor above the pool surface. Equilibrium is reached when the partial pressure of the fuel vapor above the surface equals the Clausius-Clapeyron pressure

$$p_{cc} = p_0 \, \exp \left[-\frac{h_v M_f}{\mathcal{R}} \left(\frac{1}{T_s} - \frac{1}{T_b} \right) \right] \tag{28}$$

where h_v is the heat of vaporization, M_f is the relative molecular mass, T_s is the surface temperature, and T_b is the boiling temperature of the fuel [20].

For simplicity, the liquid fuel itself is treated like a thermally-thick solid for the purpose of computing the heat conduction. There is no computation of the convection of the liquid within the pool.